



# Impedius: A Signal-Space Multiplexing Technique Using Individual Elements of Impedance for Chained Passive Sensors

Bhaskar Dutt

Department of Computer Science  
University of Copenhagen  
Copenhagen, Denmark  
bd@di.ku.dk

Daniel Ashbrook

Department of Computer Science  
University of Copenhagen  
Copenhagen, Denmark  
dan@danielashbrook.com

Yixuan Chen

Department of Computer Science  
University of Copenhagen  
Copenhagen, Denmark  
djh760@alumni.ku.dk

Valkyrie Savage

Department of Computer Science  
University of Copenhagen  
Copenhagen, Denmark  
vasa@di.ku.dk

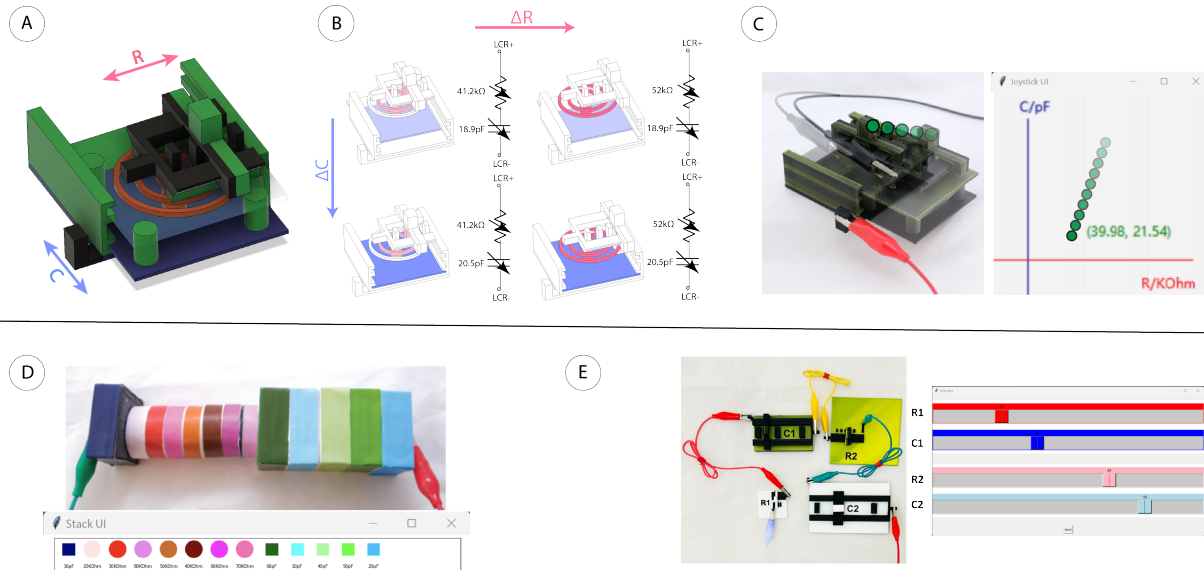


**Figure 1:** Impedius uses different elements of impedance to sense multiple interactions in a single line containing no active components. For example, a joystick (A, B, C) where one axis's motion adjusts resistance through lengthening a resistive coil (red) and the other's adjusts capacitance through overlapping two capacitive plates (blue) can control a 2D point using only one wire in and one wire out. Impedius also enables sensing the identity of stacked blocks with different resistive and capacitive signatures (D), and having several individually identifiable sliders in a single circuit using only two signals (E).

## Abstract

Commercial touch input devices sense changes in capacitance (C), resistance (R), and inductance (L), but aggregate these into a single, complex quantity: impedance. Commercially available LCR meters, however, can report the individual elements of impedance. We use

this capability to introduce Impedius, a signal-space multiplexing technique. With Impedius, we create and sense multiple static values and continuous changes in the R and C values within a single circuit by manipulating capacitance and resistance *individually*. Further, we explore 3D printing as a method to create predictable resistance and capacitance values via geometric and printer setting manipulation, and offer a software tool that generates components with desired R and C values. Based on 96 samples, our printed passive components have error  $\mu = 4.63 \text{ pF}$ ,  $\sigma = 1.68 \text{ pF}$  (capacitors) and  $\mu = 13.85 \text{ k}\Omega$ ,  $\sigma = 5.59 \text{ k}\Omega$  (resistors). We demonstrate multiple interactive example applications with our components, highlighting the opportunities for signal-space multiplexing.



This work is licensed under a Creative Commons Attribution International 4.0 License.

TEI '25, March 04–07, 2025, Bordeaux / Talence, France

© 2025 Copyright held by the owner/author(s).

ACM ISBN 979-8-4007-1197-8/25/03

<https://doi.org/10.1145/3689050.3704949>

## CCS Concepts

- Human-centered computing → Interaction devices.

## Keywords

signal-space multiplexing, impedance, 3D printing, LCR meter, passive electronics, chained sensing, sensing techniques

### ACM Reference Format:

Bhaskar Dutt, Yixuan Chen, Daniel Ashbrook, and Valkyrie Savage. 2025. Impedius: A Signal-Space Multiplexing Technique Using Individual Elements of Impedance for Chained Passive Sensors. In *Nineteenth International Conference on Tangible, Embedded, and Embodied Interaction (TEI '25), March 04–07, 2025, Bordeaux / Talence, France*. ACM, New York, NY, USA, 11 pages. <https://doi.org/10.1145/3689050.3704949>

## 1 Introduction

Touch input devices like smartphones and tablets have become ubiquitous. What these devices lack in terms of tangible feedback [24], they make up for with their powerful and flexible built-in sensing technology. This has provided an opportunity for researchers to explore input devices that, in lieu of *actively* creating and sensing active electrical impulses, *passively* control the capacitive signals emitted and sensed by these existing, omnipresent devices. Prior work in HCI has explored this technique to 3D print objects enabling rich user input [7, 38, 40]: these create a change in touch devices' sensed capacitance through interaction between a printed 3D object's design and the user's own body. Such objects, when placed on a commercial touchscreen, generate unique signatures representing placement, stacking, bending, and more, and which can be distinguished through the location, shape, or magnitude of the signals reported by the touch device.

The reported signal from these devices is an aggregated quantity called *impedance*, comprising inductance (L), capacitance (C), and resistance (R) into a single, complex quantity [18]. This means that changes in capacitance (as explored in the works above) or changes in resistance (as explored by Ohmic Touch) are indistinguishable from each other.

Although they *encode* interaction into capacitive or resistive changes, by *measuring* interaction via a single aggregated quantity, these prior passive input devices require an individual circuit (or other connection to the touch-sensing device) for each unique user input they wish to sense. This concept, known as space-multiplexing, means that passive input devices must choose between a small footprint or many inputs. Another alternative, time-multiplexing, enables sensing multiple interactions by observing a single signal's change over a period of time (as in, e.g., I<sup>2</sup>C communication), but this approach incurs a tradeoff between speed (latency) and input richness.

It is, however, possible to independently detect changes in the individual elements of impedance via an LCR meter. We use this capability to enable Impedius: a *signal-space* multiplexing technique that relies on precisely controlling separate quantities within the aggregated quantity of impedance. Signal-space multiplexing allows stacking and interpreting multiple signals within a single aggregate signal, without requiring additional space or additional time to differentiate them: using this technique, we can create and sense multiple static values and continuous changes within a single circuit

by manipulating capacitance and resistance both individually and in concert. Because of the physical interrelationship between capacitance and inductance (discussed in Section 3), we focus only on C and R, ignoring L. In figures throughout this paper, we represent **resistors in warm colours** and **capacitors in cool colours**.

Impedius uses a commercially available handheld LCR meter to demonstrate single-circuit sensing of multiple input components in series. To both precisely control component electrical characteristics and add tangible interactive features, we 3D print capacitors and resistors. Printed capacitor and resistor values depend both on material and designed geometry. We report the results of basic experiments relating 3D model dimensions to measured C and R values. In spite of 3D printers' non-homogenous deposition behavior, component values can be predicted within  $4.63 \pm 1.68 \text{ pF}$  (capacitors) and  $13.85 \pm 5.59 \text{ k}\Omega$  (resistors).

We further show how these results enable our design tool, which generates printable components with desired values. While our proof-of-concept implementation demonstrates the sensing technique, we do not deeply explore embedding these components in tangible 3D printed input devices; however, our tool would make such a thing possible.

To demonstrate the utility of signal-space multiplexing, we explore the electrical theory of impedance and show a series of use cases for our passive components. We use R and C together as independent static or variable signals, as well as using the two in a dependent configuration for error correction on a single input. We also highlight stacking single signals to re-implement classic passive devices with additional features and fidelity.

To summarize our contributions:

- (1) We propose Impedius, a sensing technique based on signal-space multiplexing using individual elements of impedance measured through an LCR meter
- (2) We demonstrate fabricating capacitor (C) and resistor (R) components through a 3D printer, and encapsulate our findings into a design tool for predictable custom components
- (3) We showcase passive, interactive input devices that provide novel functionality over existing techniques (e.g., expanded stacking, stacked continuous inputs, multi-signal error correction), while requiring only a single circuit connection.

## 2 Related Work

Our work relates to prior work in manipulation and design of electrical signals using passive components and devices, as well as 3D printing objects with embedded sensing.

### 2.1 Rapid prototyping passive electrical components

Passive components, including resistors, capacitors, and inductors, are the foundational building blocks of electrical engineering. Together with integrated circuits, they comprise in the various electronics in daily use. Researchers from various disciplines have explored creating to-order passive components (resistors, capacitors, and inductors) using accessible rapid prototyping technologies, targeting use cases such as wireless sensing [45] and custom circuit making [10, 46] with Fused Filament Fabrication (FFF) printers.

Different designs have been explored, including parallel plate capacitors [1, 22] and rolled capacitors [4]. Impedius goes beyond print-to-order to offer *interaction* with such components enabled through exploration of electrical theory.

## 2.2 Capacitive and other passive sensing methods

The seminal work Diamond Touch introduced multitouch capacitive sensing predicated on the model of a human body as an RC (resistance + capacitance) circuit component [9]. It relied on time-division multiplexing, while later touch devices instead use frequency-division multiplexing (where electrical signals of multiple frequencies are overlaid, enabling faster or richer response to user touch events) [28]. Frequency-division multiplexing is a subtype of signal-space multiplexing; it stacks frequencies of AC signal for FFT analysis, while we stack elements of impedance.

As more multitouch sensors have been built into our environments, researchers have explored extending their capabilities through developing novel devices that piggyback on them. This has been extensively explored in the context of “capacitive” touch input devices: the simplest methods extend a device’s active touch area through specially designed wires that can be 3D printed [5, 23, 38], inkjet printed [12], vinyl cut [36], or rearranged from off-the-shelf materials [7]. Richer capacitive inputs can be enabled through objects that change their signatures in response to bending [40], rotation [2, 42], or triangulation of multiple signals [41], and overall impedance can be used to sense user identity or object manipulation [43]. As noted, Ohmic-Touch discovered that touch devices actually report impedance, and so explored off-the-shelf resistive components to modify the signals of these devices [18]. These works create single-component building blocks that can be combined and sensed individually or together using our technique.

While researchers have explored overall impedance for sensing user identity and object manipulation, or have generated time-multiplexed signals for richer input, as far as we are aware, no other exploration has tackled the interactive possibilities of multiple individual components of impedance through signal-space multiplexing. Similar in spirit are works that manipulate R and C for time-domain sensing. Bae et al. explored RC delay as an underlying technique to visualize network data physically [3]. RC delay-based sensing measures different time delays in a circuit, which can be controlled through specific R and C signatures. Bae et al. use this time-domain signal with designed resistances to sense touch at various locations on a printed object; here we use signal-domain multiplexing with R and C modifications to sense rich signals that go beyond binary touch. Similarly, Touché uses time-domain signals to sense rich touch inputs, which enables varied inputs but also requires training machine learning models and works in the time domain to do the sweep. Others have explored alternative passive electronics, like embedded RFID/NFC components [17, 27], wireless backscatter signals [20], or electromagnetic interference [14, 29, 33], that can likewise be sensed by environmental sensors: while they offer rich inputs, these techniques rely on rarer sensor types and still use time-domain multiplexing.

## 2.3 Geometry- and material-based signal transformation

One of the biggest benefits of 3D printers is their ability to create intricate and complex geometries. Researchers have used this capability to embed wide-ranging sensing capabilities directly within 3D-printed objects, sometimes by adapting new, printed objects to actuate existing, unprinted ones [32] or by enabling embedding of off-the-shelf electronics [8, 16]. Another strategy involves replacing electronic sensors with structural (plastic) sensing. This type of technique can be seen in the various systems using metamaterials’ behaviours for sensing [11, 19]; closer to our work are systems that proxy signals through 3D printed objects’ geometries and onto alternative sensors, as described by Savage [37]. While many of these latter techniques were discussed under the passive electrical section above [2, 5, 7, 23, 38, 40–42], there are other possible sensing mechanisms. For example, Han et al. use 3D printing to create devices that convey touch or twist inputs—in the form of air pressure changes—down to a force-sensitive touchpad [15]. Printed Optics uses light as a medium to proxy sensing in a passive manner through printed objects [44]. Acousturments manipulates sound in printed tubes [26], while A Series of Tubes more generally suggests using various media inserted post-print for this signal-proxying task [35]. The key idea of embedding structures into digitally fabricated objects that manipulate a senseable characteristic in a predictable fashion is not new: Impedius takes inspiration from these works and explores the interactive possibilities of signal-space multiplexing in impedance, which we support with 3D printed-to-order passive components.

## 3 Electrical Theory of Impedius

Impedance ( $Z$ ), a fundamental concept in electrical circuits, represents the collective resistance within a circuit and is comprised of three elements: capacitance ( $C$ ), resistance ( $R$ ), and inductance ( $L$ ) (see Table 1 for a summary of symbols and units). Capacitance measures the ability of two conductors, separated by some distance, to store an electrical charge. Resistance measures how much a conductor resists the flow of electricity. Inductance measures a circuit’s capability to store magnetic energy. Each of these properties have physical components which are used in electrical circuits: capacitors, resistors, and inductors. These are referred to as “passive electrical components” because they do not provide electrical power, but rather modify the power flowing through the circuit. Resistance is the simplest property, as it behaves the same in DC and AC circuits, while capacitance and inductance demonstrate frequency-dependent reactance (analogous to resistance) when connected to AC circuits. The equation for the magnitude of the total impedance in a circuit therefore takes the signal frequency  $f$  into account:

$$|Z| = \sqrt{R^2 + \left(2\pi fL - \frac{1}{2\pi fC}\right)^2} \quad (1)$$

Note that  $L$  and  $C$  have opposite contributions to the total impedance, so adding inductance to a circuit will reduce the effect of capacitance and vice-versa.

Modern touch sensing circuits (such as those in smartphone screens) typically use pairs of electrodes, with one electrode in a pair transmitting a high-frequency electrical signal which the other

Symbol	Name	Unit	Component symbol
Z	impedance	$\Omega$ (ohm)	N/A
L	inductance	H (henry)	
C	capacitance	F (farad)	
R	resistance	$\Omega$ (ohm)	
f	frequency	Hz (hertz)	N/A

**Table 1: Summary of electronic terms, symbols, and names used in this document. Variable versions of the circuit components are rendered with an arrow across their design (e.g., ).**

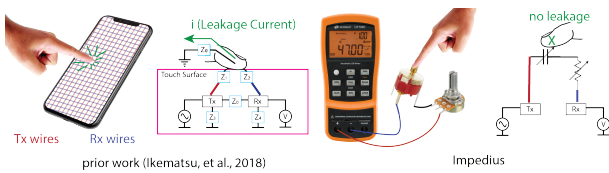


**Figure 2: Impedijs (right) relies on closed-loop sensing on a single circuit, which makes it less susceptible to both noise and touch-based interactions than the grid of transmit ( $T_x$ ) and receive ( $R_x$ ) wires in a smartphone touch sensor (left, circuit figure adapted from [18]).**

receives. A human body approaching the electrode pair absorbs some of the transmitted signal [13]. The path through the Rx and Tx electrodes has impedance [25] which varies via changes in the capacitive coupling between the body and electrode (C). Touch controllers detect how current (I) is attenuated by the change in impedance (due to Ohm's law,  $I = V/Z$ ). Although the amount of attenuation in I is due to the change in the capacitor created by the human body and the electrode (primarily the distance between the two), this change in measured current is affected by *any* change in impedance, including those due to changes in L or R [18].

In contrast to touch controllers, LCRs precisely record the individual changes occurring within the inductive (L), capacitive (C), and resistive (R) components of the circuit; they measure a circuit's impedance by supplying an AC signal at a specific frequency and comparing its response to known values. This capability allows the meter to detect, for example, the individual C and R values of a capacitor and a resistor connected in series. If the values of one or both components change, the readings from the meter will reflect this fact. We call this "signal-space multiplexing," as the input components in question need only be connected in a simple circuit to the LCR meter and can be distinguished through orthogonal changes in signal: they do not require individual circuits per input (space multiplexing), nor do they require communication protocols on the wire (time-based multiplexing) (see Figure 2).

## 4 Interactions

Impedijs takes advantage of signal-space multiplexing to sense multiple 3D-printed interactive components connected in series,

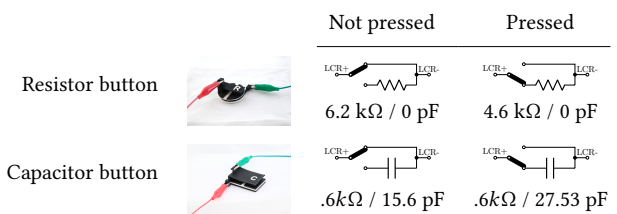


**Figure 3: Buttons attached individually to the LCR meter, showing readings for each when pressed and not pressed. (Note that when pressed, each button shorts the connection, effectively disconnecting the printed component.)**

enabling a higher number of points of interaction with less complexity than the previous approaches described in Section 2. We illustrate the advantages of this method with several examples.

### 4.1 Detecting interaction

Our first example shows how we can detect simple interactions with 3D-printed components. Figure 3 illustrates two buttons printed with conductive and non-conductive PLA. One button contains a printed capacitor while the other incorporates a printed resistor. When a button is not pressed, the circuit makes a direct connection between the two terminals of the LCR meter, so the impedance consists solely of the R resulting from the conductive filament's inherent resistance.

When one of the buttons is depressed, the circuit then includes the component embedded into the button body. The meter readout then reflects the amount of resistance and capacitance added by the component. By examining the values, it is simple to detect which of the two buttons is attached to the meter and when it is pressed.

### 4.2 Chaining using different elements of impedance

Because the LCR meter is able to separate the three elements of impedance, we can trivially connect the buttons in series (Figure 4). Now with only a single circuit, we have two buttons which can be independently and simultaneously detected: when the "R" button is pressed, the R part of impedance increases, and when the "C" button is pressed, the C part *decreases* (due to the reciprocal in Equation 1). When both are pressed, both the R and C parts change. Because L and C have opposite effects on the total magnitude of impedance (Equation 1), with Impedijs we use only resistors and capacitors, and leave the exploration of inductors to future work.

### 4.3 Chaining more than two passive components

Multiple R or L components in a series circuit are *additive* (Equation 1). When measured separately by the LCR meter via a time-domain signal, we can thus easily identify the value of an added inductive or resistive component by the change in the L or R value. For example, if we add an unknown resistor to a circuit that includes a  $10k\Omega$  resistor for a total R of  $35k\Omega$ , we can trivially calculate that the new resistor's value is  $25k\Omega$ .

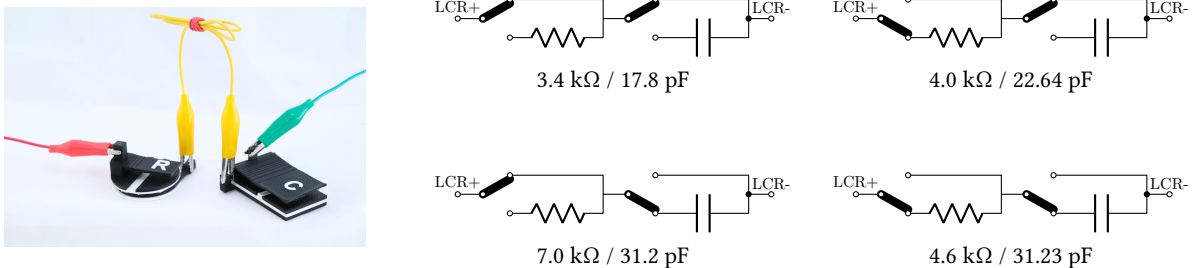


**Figure 4:** A resistor button and a capacitor button in series have four possible pressing configurations. Each of these readings shows a unique R and C reading combination. (Note that when pressed, the button shorts each connection, effectively disconnecting the printed component.)

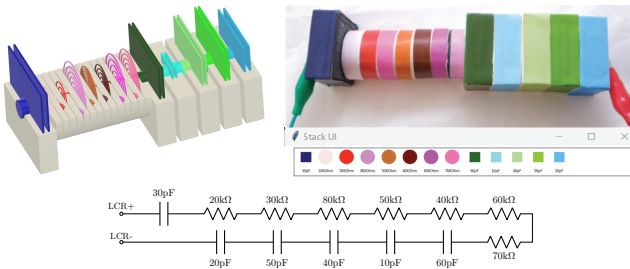


**Figure 5:** By embedding resistor coils and capacitor plates of various values into blocks (top left), we can print geometries that can be uniquely distinguished as they are added to a component stack (top right). Here we stack 13 blocks with non-overlapping IDs in R and C. Our stacks' sizes are theoretically infinite and limited only by the precision and range of the LCR meter itself, rather than physical design complexity ([27] max 12, [7] max 3).

Connecting multiple capacitors in series is slightly more complicated: the reciprocal of the circuit's total capacitance is equal to the sum of the reciprocals of the capacitances in it, i.e., the total capacitance reduces with additional capacitors:  $1/C_{total} = 1/C_1 + 1/C_2 + \dots + 1/C_N$ . Thus, if we add an unknown capacitor to circuit that includes a  $120\text{pF}$  capacitor for a total C of  $100\text{pF}$ , we then solve  $1/100 = 1/120 + 1/x$  to get the value of the added capacitor as  $600\text{pF}$ . While this calculation is straightforward, it points out that as we add capacitors, the overall total capacitance decreases, and could potentially drop below the lowest value that the LCR meter can measure. We did not experience this during our research, but in future systems it may be a consideration.

In order to avoid ambiguity when adding components, we wait for the readings to stabilize after each addition to clearly observe the new value. Figure 5 illustrates multiple R and C components chained together. The resistors have 7 values, ranging from  $20\text{--}80\text{ k}\Omega$ , with a step size of  $10\text{ k}\Omega$ , while the capacitors have 6 values ranging from  $10\text{--}60\text{ pF}$ , with a step size of  $10\text{ pF}$ . With all components connected, the LCR meter reads  $R_{total} = 350\text{k}\Omega$  and  $C_{total} = 4.1\text{pF}$ . If we know which components are available, we can unambiguously determine which are involved in the circuit.

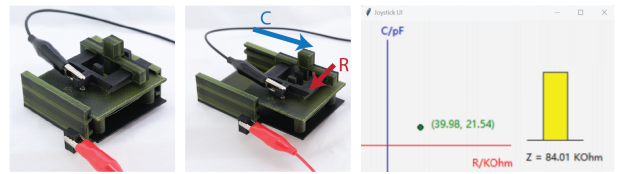


**Figure 6:** An Impedius joystick, which uses resistance values for x input and capacitance values for y input (left). Resistance is sampled on three points along a resistive spiral, while capacitance is changed by offsetting one plate of the capacitor via sliding. This enables 2D input, where impedance alone could not (right).

#### 4.4 Sensing interaction via variable component values

Using multiple components with different C or R elements allows us to sense the presence or absence of those components. We extend this principle to combine multiple values for a single part of impedance in one component, so that physically interacting with the component changes that component's C or R in a predictable way. Figure 6 illustrates this idea via a 3D-printed 2D joystick, where movement in one axis changes the R value, and movement in the other axis changes the C value. As with the previous examples, the C and R values are able to be separately detected by the LCR meter, allowing the two axes of the joystick to be read by a single circuit connection.

#### 4.5 Sensing interaction with multiple components

The limitation of sensing interaction by continuously varying one element of impedance is that additional components will be indistinguishable from each other; with two continuous R inputs, for example, it becomes impossible to tell which input is being manipulated (or if, indeed, both are being manipulated at the same time).

To solve this problem, we use the strategy described in Section 4.3, where each component has its own unique series of discrete steps of an individual size and/or within an individual range

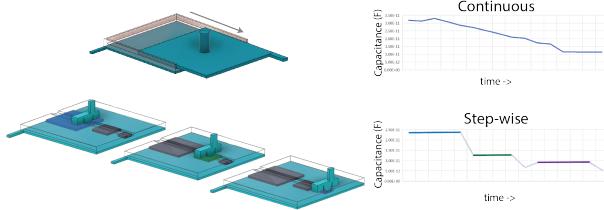


**Figure 7:** Continuous changes in capacitance created by continuous change in overlapped area between two plates work well when a single variable capacitor is in a circuit (top), but step-wise changes, where the wiper “selects” one of several possible values—here seen as a blue, green, or purple top plate in the capacitor—are required to accommodate more than one (bottom).

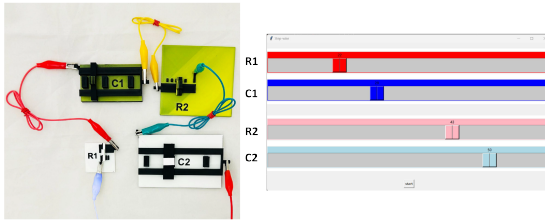


**Figure 8:** Impedium supports multiple variable inputs in a single element, for example two R sliders and two C sliders in series (left), by adding uniquely sized, stepped changes to distinguish individual components’ positions (right).

of values (Figure 7). For example, to include two variable capacitors in a single device, the first could have step sizes of 1.5pF and the second could have steps of 2pF. In this way, interactions show “jumps” of specific sizes which are linked to the component being manipulated (Figure 8).

#### 4.6 Manipulating the elements of impedance

To detect the operation of physical controls as described above, manipulation of the controls must result in predictable and detectable changes to the individual elements of impedance. While factory-produced inductors, capacitors, and resistors are readily available with wide ranges of values, *variable* capacitors and inductors are relatively uncommon. To enable interaction, we need not only variable electrical components, but also components with specific step sizes to allow detecting which component is being changed.

The values of L, C, and R are governed by well-understood geometric and material properties. By using standard printable materials but allowing the geometry to be changed by interaction, we design and 3D print tangible components that accomplish this goal.

The inductance L of a coil is defined as  $L = \mu(N^2 A)/l$ , where  $\mu$  is the magnetic permeability of the material in between the coil turns,  $N$  is the number of turns,  $A$  is area of the encircled coil, and  $l$  is the length of the coil. Note that we did not experiment with inductance in Impedium; we provide its high-level information for completeness and future work. The capacitance of a pair of

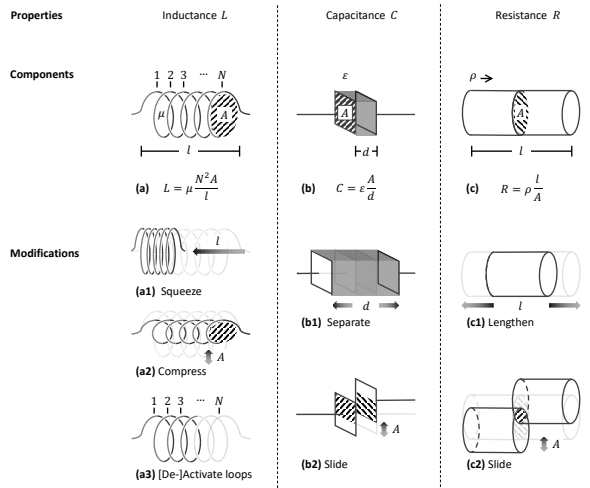


**Figure 9:** The geometric components of L, C, and R, and how they can be manipulated statically and interactively.



**Figure 10:** Our prediction toolkit runs as a script inside Fusion 360 (left) and generates printable resistors and capacitors (center) whose values closely adhere to desired values (right).

parallel plates is  $C = \epsilon A/D$ , where  $\epsilon$  is the permittivity of the dielectric material between the plates,  $A$  is the overlapping area of the plates, and  $D$  is the distance between them. A material’s resistance is  $R = \rho L/A$ , where  $\rho$  is the resistivity of the material,  $L$  is its length, and  $A$  is its cross-sectional area. Treating  $\mu$ ,  $\epsilon$ , and  $\rho$  as invariant properties of the materials we print with allows us to utilize geometry to tailor the L, C, or R values of a given component (Figure 9).

These same variables that can be controlled in manufacture can also be manipulated through motion for sensing dynamic interactions (Figure 9). For example, we can modify resistance by changing the length of a circuit’s path through a printed resistor, or we can control the overlapping cross-sectional area of two serially connected conductors to “pinch” the current flow through it [18]. Modifying the area of overlap between two plates, or the distance between them, can generate different capacitance, as extensively explored in previous research [38, 40]. Inductance, a slightly more complicated quantity, could be interactively controlled by activating or deactivating loops in a device—thus generating additional “turns”—changing the overall length of the coil, or compressing the coil and effectively changing the overall area under the coil [30].

**Table 2: Summarized experimental results for printed resistors and capacitors comparing their geometric components to resulting values.**

Manipulated Attribute	Component	Result	R <sup>2</sup>	p> t	F-statistic
Length	Resistor	Proportional Change	0.758	<.001	75.21
	Resistor	Inverse Proportional Change	0.898	0.052	17.6
Cross-sectional Area	Capacitor	Proportional Change	0.984	<.001	298.5
	Capacitor	Inverse Proportional Change	0.989	0.068	86.02

## 5 Impedius: Prototype System Implementation

### 5.1 Printing predictable R and C components

Given the non-homogeneous nature of 3D printed objects, we wanted to confirm that we can predict values of R and C components using their geometry. We thus collected data on both types of components to find their material characteristics ( $\rho$  and  $\epsilon$ ), and implemented a script that can create geometry with desired resistances and capacitances for designers to work with in their 3D models.

All prototypes were modeled in Fusion 360 and sliced using Ultimaker Cura 5.4.0 or Bambu Studio 1.7.4.52 with layer height 0.2 mm and solid infill, then fabricated on Ultimaker S3 or Bambu Lab X1-Carbon, equipped with 0.4 mm nozzle. Samples were printed in Conductive PLA (Protopasta), PLA (Bambu Lab “PLA Basic”, Ultimaker “Ultimaker PLA”), and TPU+PLA (Bambu Lab “Support For PLA”), and all measurements were performed using a Keysight LCR meter model U1733C with 100 kHz frequency as the input signal—this provided the most stable readings (see Figure 10). Our most important results are summarized here (see Table 2): even non-homogenous, 3D-printed components are predictable and adhere to the expected equations within tolerances similar to those that are mass-produced. We also found no notable differences in the behaviour of components printed on our two machines.

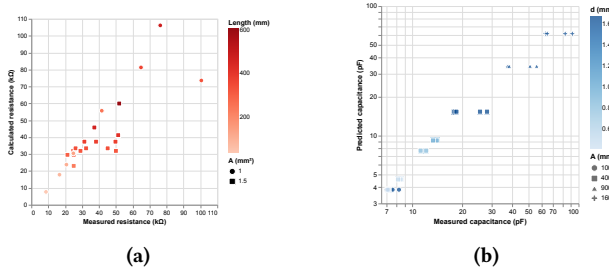


**Figure 11: Measured versus predicted values for test resistors (a) and capacitors (b).**

**5.1.1 Exploring geometric parameters of resistance.** We printed 40 spiral-shaped prototypes to explore the effects of geometry parameters on resistance, as this design is more space-efficient than a linear one and thus enables a wider range of resistances to be printed in the same volume. In a spiral resistor, D (inner diameter), R (number of revolutions), P (pitch) and S (section size) together decide the overall length of the spiral,  $l = \pi * R * (D/2 + R * P + S)$ , and S also decides the cross-sectional area,  $A = S^2$  (see Figure 12). We conducted a series of controlling variable experiments on these four parameters: D(3–24 mm), R(2–16), P(2–16 mm), and S(0.5–4 mm),

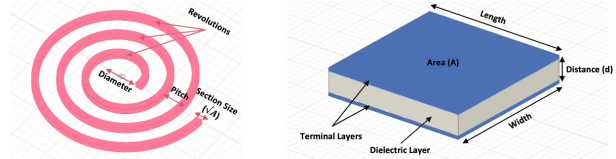


**Figure 12: Geometric parameters of our tested resistor (left) and capacitor (right) models.**

where each step doubles the previous figure. Regression analysis showed that resistance has a linear relationship with length and reciprocal of cross-sectional area, consistent with the equation for Resistance (see Table 2). We also measured that our resistors have 13 pF of capacitance, and our capacitors have 1.7 kΩ resistance.

**5.1.2 Exploring geometric parameters of capacitance.** Our capacitors are classic parallel plate capacitors (see Figure 12). Since the capacitance of a parallel plate capacitor is theoretically decided by the overlapping area and the distance between two terminals, we tried to explore the relationships between capacitance and its geometry parameters, including the overlapping area (Length \* Width) and the distance between terminals. We printed 5 batches of prototypes modifying Length, i.e. area, (10mm – 80mm), as well as 3 batches testing distance (0.6mm – 2.4mm). We printed 4 identical samples in each batch, and each batch doubled the measurement of the previous. We then measured the capacitances of our prototypes and found a significant linear relationship with the overlapping area and the reciprocal of the height (see Table 2). Our capacitors have a small amount of resistance, approximately equal to that of printed wires made from our conductive material.

**5.1.3 Modeling R and C based on geometric parameters.** Given the collected data, we modeled resistance and capacitance based on geometric inputs using the general physical formulas governing their characteristics.

We performed linear regression with 5-fold cross-validation in both cases. For resistance, we found our printed mean resistivity  $\rho$  to be  $0.215\Omega/mm$ , with an intercept term (representing irreducible resistance created by the connection to the measuring device) of  $8.227k\Omega$ . The mean percentage error was  $MPE = 25.93\%$ , with standard deviation  $\sigma = 13.75\%$ , and the mean absolute error was  $\mu = 13.85k\Omega$ , with  $\sigma = 5.59k\Omega$ . Also, a linear regression (see Table 2) on the printed resistors found the overall fit to be  $r^2 = 0.758$ ,  $p < .001$  for length and  $r^2 = 0.898$ ,  $p = 0.05$  for cross-sectional area. For capacitance, our printed  $\epsilon$  was  $0.023pF/mm$ , with an intercept term (representing irreducible capacitance due to imperfect fusion of adjacent print layers) of  $5.780pF$ . The mean percentage error was  $MPE = 20.08\%$ , with  $\sigma = 13.81\%$ , and the mean absolute error was  $\mu = 4.63pF$ , with  $\sigma = 1.68pF$ . The linear regression (see Table 2) on the capacitors found the overall fit to be  $r^2 = 0.984$ ,  $p < .001$  for area and  $r^2 = 0.989$ ,  $p = 0.068$  for distance. The results indicate that we could fabricate and predict the resistors and capacitors in a stable and precise approach. We also experimented with neural networks for fitting, but they did not outperform our linear models, so we continued with the simpler solution.

**5.1.4 Post-processing for printed geometry.** The filaments we use in our printed components have a suitable internal resistivity, but their *terminal* resistance, i.e., the resistance created by connecting them to a non-printed or separately printed object, is very high. In order to mitigate this, we experimented with various conductive paints, per manufacturer suggestions<sup>1</sup>. Based on ease of application and durability, we add Bare Conductive's Electric Paint<sup>2</sup> to all surfaces of printed objects where they contact other printed objects, e.g., sliders (see Figure 8, left).

## 5.2 Generating geometry for predictable R and C

We encapsulated our knowledge from above in a toolkit for Autodesk's Fusion modeling program. The toolkit accepts as input a desired resistance or capacitance value from the user and generates geometry to suit. To manage the size of the generated model and also to shorten the search time, we use a randomized algorithm to generate the parameters separately within the range bounded by the size of the printing plate, and output the first parameter set that fits the desired R/C value and other physical requirements, such as the pitch being larger than the section size (see Figure 10a).

After geometry is generated, users can appropriate it for static identity objects, or as part of various tangible input components (like the buttons and sliders showcased here). Including stepped geometry into a component requires that users generate multiple subgeometries for integration (see Figure 7).

## 5.3 Sensing with Impedius

Our LCR meter offers USB-based serial communication. We use this connection with the default parameters, enabling us to write generic python scripts that accept individual L, C, and R values over serial (see Figure 10). The Keysight U1733C has 1 Hz reporting, with each report containing all requested measurements.

## 6 Discussion and Limitations

Impedius represents a first exploration into using multiple electrical signal elements for independent sensing tasks through signal-space multiplexing. Our particular implementation of the system has a number of limitations.

Impedius requires individual reporting of L, C, and R components, which as discussed in Section 3 is currently not available in commercial touch controllers. We get readings via serial port from a handheld LCR meter, which is a device that has been engineered for precision rather than interactive speeds. As such, we get updated information at just 1 Hz (it is possible to overclock to 3 Hz<sup>3</sup>) and on only one line of chained components. A customized LCR circuit could offer higher read rates and multiple parallel connections, further increasing the number of senseable components. In theory, the de-aggregated impedance data that Impedius utilizes could be reported by the touch controller of common devices like smartphones.

<sup>1</sup><https://www.multi3dmc.com/faqs/>

<sup>2</sup><https://www.bareconductive.com/products/electric-paint>

<sup>3</sup>using FREQ 100k <https://community.keysight.com/forums/s/question/0D52L00005IdpcBSAR/u1732c-scpi-commands>

The human body also, of course, has inherent electrical properties. This could disturb LCR meter readings, but as LCR meters are generally designed to measure closed-circuit designs as compared to the open-circuits touch controllers focus on, they are generally less sensitive to body noise. This closed-circuit design also means that our interfaces can be operated with gloves or other hand-wear on, since sensing their state does not rely on shunting current through a human body. Body-based interference, if it appears in future work, could be mitigated through insulating or shielding the components to be sensed from the user's body.

## 6.1 Components

Our printed, predictable components represent a step towards general, configurable, passive electrical components, but suffer from some inaccuracies due to the maker-class machines we use and limitations of the material (e.g., the need to post-process with paints for reduced terminal resistance). Our tolerance values (20–25 %) are not dissimilar to those of cheap mass-manufactured components (typically 10%), but we note that the Impedius technique itself can be used to counteract manufacture errors: by creating components where R and C give the same information, we can error-correct. For example, we built a slider which uses both R and C to sense the same motion, increasing robustness (see Figure 13). Stopping mid-print to insert off-the-shelf components or calibrate and manipulate G-code<sup>4</sup> are also opportunities to improve component tolerances if the use case and designer's expertise allow it.

When thinking about how to use Impedius-powered components, we suggest that future designers consider the physical interactions they wish to sense (using, e.g., Card, et al.'s design space [6]) and map those motions to the kinds of modifications that lead to signal changes in C, R, or L (Figure 9). The laws that govern the signals' manipulation along with consideration of how "busy" a single element of the signal space of a design already is (i.e., how many interactions are being mapped there) may help in deciding which element to leverage. A future version of the design tool we prototyped could also enable designers to visualize or automatically fit the sensing they want into the range offered by their sensing device by optimizing step sizes of components in a device to be printed.

## 6.2 LCR Meter

A limitation of our current implementation is the reliance on an off-the-shelf LCR meter, which prevents easy integration of the Impedius technique into standalone objects. However, multiple examples exist of hobbyist-level LCR meters<sup>5</sup><sup>6</sup><sup>7</sup> which offer smaller sizes and thus inspiration for a more-integrated solution. Speed-wise, they could improve Impedius's performance, as they can be designed to offload expensive computation to other devices in a way the off-the-shelf meter does not. The drawback to these solutions is reduced accuracy; while the Keysight LCR meter we used in our implementation reports values with 0.2% accuracy, hobbyist LCR meters report about 1% accuracy at best. A lower accuracy from the measurement instrument, in combination with the variability

<sup>4</sup><https://community.octoprint.org/t/can-i-edit-the-currently-printed-gcode/59667/2>

<sup>5</sup><https://github.com/wschorum/TeensyLCR>

<sup>6</sup><https://adilmalikn.wordpress.com/2019/07/07/low-cost-high-accuracy-stm32-ftlcr-meter/>

<sup>7</sup><https://jyetech.com/m162-lcr-meter/>

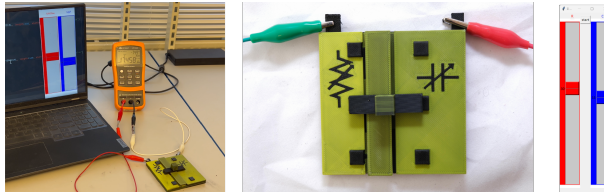


**Figure 13:** By measuring the same interaction with multiple elements of impedance, we can overcome imperfections in our component value prediction script. This slider uses both R and C for variable sensing on the same track.

inherent in 3D printing, suggests future work in exploring how variations in factors such as temperature, speed, layer height, and component orientation affect the variance of measured R and C values.

Including multiple LCR circuits in a system could also enable sensing even more inputs, or creating Tx/Rx grids.

## 7 Future Work

Previous research has demonstrated a wide range of mechanical designs for fabricated input devices—especially those using the capacitive part of impedance—enabling, for example, sensing touch [39], force [40], or rotation [2]. Similar design techniques could also be incorporated in the Impedius design tool, along with support for specific application areas such as character animation [21] or input devices [34].

While we did initial tests 3D printing inductors, the inverse relationship between L and C (Section 3) means it is only practical to manipulate one of them in a given component chain if we want accurate, absolute sensing of individual elements. Due to the large body of previous experiments around capacitance-based sensing [13, 39], we chose to vary C. Future work could explore the applicability of inductors in signal-space multiplexed sensing, e.g., in scenarios where magnets are involved.

Circuits composed of passive components also have other measurable features that could be of interest for interaction, such as resonant frequency (i.e., the AC frequency at which L and C balance out, making a purely resistive circuit) and transfer functions (visualized as Nyquist plots), which could be explored in future work as additional signal-space values. Frequency-dependent reactance of L and C could also be in multi-component, Touché-like swept frequency sensing [31], though this is not a signal-space characteristic.

As noted, we discretized our resistive and capacitive steps when we included more than one resistor or capacitor in a single circuit in order to distinguish their values. Future work can explore more sophisticated blending of element signatures so that, e.g., moving one slider creates an increase in a resistance and a decrease in capacitance, while moving another reduces capacitance at a faster rate, creates an increase in both elements, or modifies the phase angle of the circuit. Our predictable, 3D printable components will aid in this type of exploration.

## 8 Conclusion

In this paper, we introduced Impedius, a signal-space multiplexing technique that enables sensing multiple static or continuous input values in a single circuit by targeting specific electrical characteristics. We discussed the electrical theory underlying these capabilities and its relationship to modern devices' inbuilt touch controllers. We further explored various uses of Impedius for multidimensional input and error correction, as well as used 3D printers to create custom electrical components in a predictable manner for it.

## Acknowledgments

We would like to thank Martin Schmitz for discussion on ideas and concepts, Atul Chaudhary for help in mechanical design, and Athina Panotopoulou for aid in figure-making. This work was partially supported by a Novo Nordisk Fonden Starting Grant under grant number NNF21OC0072716.

## References

- [1] Xavier Aeby, Ryan van Dommelen, and Danick Briand. 2019. Fully FDM 3D Printed Flexible Capacitive and Resistive Transducers. In *2019 20th International Conference on Solid-State Sensors, Actuators and Microsystems & Eurosensors XXXIII (TRANSDUCERS & EUROSENSORS XXXIII)*, 2440–2443. <https://doi.org/10.1109/TRANSDUCERS.2019.8808268> ISSN: 2167-0021.
- [2] Marwa Alalawi, Noah Pacik-Nelson, Junyi Zhu, Ben Greenspan, Andrew Doan, Brandon M Wong, Benjamin Owen-Block, Shanti Kaylene Mickens, Wilhelm Jacobus Schoeman, Michael Wessely, Andreea Danilescu, and Stefanie Mueller. 2023. MechSense: A Design and Fabrication Pipeline for Integrating Rotary Encoders into 3D Printed Mechanisms. In *Proceedings of the 2023 CHI Conference on Human Factors in Computing Systems (CHI '23)*. Association for Computing Machinery, New York, NY, USA, 1–14. <https://doi.org/10.1145/3544548.3581361>
- [3] S. Sandra Bae, Takanori Fujiwara, Anders Ynnerman, Ellen Yi-Luen Do, Michael L. Rivera, and Danielle Albers Szafir. 2023. A Computational Design Pipeline to Fabricate Sensing Network Physicalizations. *arXiv:2308.04714 [cs.HC]* <https://arxiv.org/abs/2308.04714>
- [4] Nelu V. Blaž, Ljiljana D. Živanov, Milica G. Kisić, and Aleksandar B. Meničanin. 2022. Fully 3D printed rolled capacitor based on conductive ABS composite electrodes. *Electrochemistry Communications* 134 (Jan. 2022), 107178. <https://doi.org/10.1016/j.elecom.2021.107178>
- [5] Jesse Burstyn, Nicholas Fellion, Paul Strohmeier, and Roel Vertegaal. 2015. PrintPut: Resistive and Capacitive Input Widgets for Interactive 3D Prints, Vol. LNCS-9296. 332. [https://doi.org/10.1007/978-3-319-22701-6\\_25](https://doi.org/10.1007/978-3-319-22701-6_25) Issue: Part I.
- [6] Stuart K. Card, Jock D. Mackinlay, and George G. Robertson. 1991. A morphological analysis of the design space of input devices. *ACM Trans. Inf. Syst.* 9, 2 (April 1991), 99–122. <https://doi.org/10.1145/123078.128726>
- [7] Liwei Chan, Stefanie Müller, Anne Rouaut, and Patrick Baudisch. 2012. Cap-Stones and ZebraWidgets: sensing stacks of building blocks, dials and sliders on capacitive touch screens. In *Proceedings of the SIGCHI Conference on Human Factors in Computing Systems (CHI '12)*. Association for Computing Machinery, New York, NY, USA, 2189–2192. <https://doi.org/10.1145/2207676.2208371>
- [8] Claudia Daudén Roquet, Jeeeon Kim, and Tom Yeh. 2016. 3D Folded PrintGami: Transforming Passive 3D Printed Objects to Interactive by Inserted Paper Origami Circuits. In *Proceedings of the 2016 ACM Conference on Designing Interactive Systems (Brisbane, QLD, Australia) (DIS '16)*. Association for Computing Machinery, New York, NY, USA, 187–191. <https://doi.org/10.1145/2901790.2901891>
- [9] Paul Dietz and Darren Leigh. 2001. DiamondTouch: A Multi-User Touch Technology. *Proc. UIST '01*. <https://doi.org/10.1145/502348.502389>
- [10] Patrick F. Flowers, Christopher Reyes, Shengrong Ye, Myung Jun Kim, and Benjamin J. Wiley. 2017. 3D printing electronic components and circuits with conductive thermoplastic filament. *Additive Manufacturing* 18 (Dec. 2017), 156–163. <https://doi.org/10.1016/j.addma.2017.10.002>
- [11] Jun Gong, Olivia Seow, Cedric Honnet, Jack Forman, and Stefanie Mueller. 2021. MetaSense: Integrating Sensing Capabilities into Mechanical Metamaterial. In *The 34th Annual ACM Symposium on User Interface Software and Technology (Virtual Event, USA) (UIST '21)*. Association for Computing Machinery, New York, NY, USA, 1063–1073. <https://doi.org/10.1145/3472749.3474806>
- [12] Nan-Wei Gong, Jürgen Steinle, Simon Olberding, Steve Hodges, Nicholas Edward Gillian, Yoshihiro Kawahara, and Joseph A. Paradiso. 2014. PrintSense: A Versatile Sensing Technique to Support Multimodal Flexible Surface Interaction. In *Proceedings of the SIGCHI Conference on Human Factors in Computing Systems*

- (Toronto, Ontario, Canada) (*CHI '14*). Association for Computing Machinery, New York, NY, USA, 1407–1410. <https://doi.org/10.1145/2556288.2557173>
- [13] Tobias Grosse-Puppendahl, Christian Holz, Gabe Cohn, Raphael Wimmer, Oskar Bechtold, Steve Hodges, Matthew S. Reynolds, and Joshua R. Smith. 2017. Finding Common Ground: A Survey of Capacitive Sensing in Human-Computer Interaction. In *Proceedings of the 2017 CHI Conference on Human Factors in Computing Systems* (Denver, Colorado, USA) (*CHI '17*). Association for Computing Machinery, New York, NY, USA, 3293–3315. <https://doi.org/10.1145/3025453.3025808>
- [14] Sidhant Gupta, Matthew S. Reynolds, and Shwetak N. Patel. 2010. ElectriSense: Single-Point Sensing Using EMI for Electrical Event Detection and Classification in the Home. In *Proceedings of the 12th ACM International Conference on Ubiquitous Computing* (Copenhagen, Denmark) (*UbiComp '10*). Association for Computing Machinery, New York, NY, USA, 139–148. <https://doi.org/10.1145/1864349.1864375>
- [15] Changyo Han, Ryo Takahashi, Yuchi Yahagi, and Takeshi Naemura. 2020. Pneu-Module: Using Inflatable Pin Arrays for Reconfigurable Physical Controls on Pressure-Sensitive Touch Surfaces. In *Proceedings of the 2020 CHI Conference on Human Factors in Computing Systems* (*CHI '20*). Association for Computing Machinery, New York, NY, USA, 1–14. <https://doi.org/10.1145/3313831.3376838>
- [16] Liang He, Jarrid A. Wittkopf, Ji Won Jun, Kris Erickson, and Rafael Tico Ballagás. 2022. ModElec: A Design Tool for Prototyping Physical Computing Devices Using Conductive 3D Printing. *Proc. ACM Interact. Mob. Wearable Ubiquitous Technol.* 5, 4, Article 159 (Dec. 2022), 20 pages. <https://doi.org/10.1145/3495000>
- [17] Meng-Ju Hsieh, Rong-Hao Liang, Da-Yuan Huang, Jheng-You Ke, and Bing-Yu Chen. 2018. RFIBricks: Interactive Building Blocks Based on RFID. In *Proceedings of the 2018 CHI Conference on Human Factors in Computing Systems* (Montreal QC, Canada) (*CHI '18*). Association for Computing Machinery, New York, NY, USA, 1–10. <https://doi.org/10.1145/3173574.3173763>
- [18] Kaori Ikematsu and Itiro Saito. 2018. Ohmic-Touch: Extending Touch Interaction by Indirect Touch through Resistive Objects. In *Proceedings of the 2018 CHI Conference on Human Factors in Computing Systems* (Montreal QC, Canada) (*CHI '18*). Association for Computing Machinery, New York, NY, USA, 1–8. <https://doi.org/10.1145/3173574.3174095>
- [19] Alexandra Ion, Ludwig Wall, Robert Kovacs, and Patrick Baudisch. 2017. Digital Mechanical Metamaterials. In *Proceedings of the 2017 CHI Conference on Human Factors in Computing Systems* (Denver, Colorado, USA) (*CHI '17*). Association for Computing Machinery, New York, NY, USA, 977–988. <https://doi.org/10.1145/3025453.3025624>
- [20] Vikram Iyer, Justin Chan, Ian Culhane, Jennifer Mankoff, and Shyammath Golakota. 2018. Wireless Analytics for 3D Printed Objects. In *Proceedings of the 31st Annual ACM Symposium on User Interface Software and Technology* (Berlin, Germany) (*UIST '18*). Association for Computing Machinery, New York, NY, USA, 141–152. <https://doi.org/10.1145/3242587.3242639>
- [21] Alec Jacobson, Daniele Panozzo, Oliver Gläser, Cédric Pradalier, Otmar Hilliges, and Olga Sorkine-Hornung. 2014. Tangible and modular input device for character articulation. *ACM Trans. Graph.* 33, 4 (July 2014), 82:1–82:12. <https://doi.org/10.1145/2601097.2601112>
- [22] Nebojsa I. Jaksic and Pratik D. Desai. 2019. Characterization of 3D-printed capacitors created by fused filament fabrication using electrically-conductive filament. *Procedia Manufacturing* 38 (Jan. 2019), 33–41. <https://doi.org/10.1016/j.promfg.2020.01.005>
- [23] Kunihiro Kato, Kaori Ikematsu, and Yoshihiro Kawahara. 2020. CAPath: 3D-Printed Interfaces with Conductive Points in Grid Layout to Extend Capacitive Touch Inputs. *Proc. ACM Hum.-Comput. Interact.* 4, ISS (Nov. 2020), 193:1–193:17. <https://doi.org/10.1145/3427321>
- [24] Scott R. Klemmer, Björn Hartmann, and Leila Takayama. 2006. How Bodies Matter: Five Themes for Interaction Design. In *Proceedings of the 6th Conference on Designing Interactive Systems* (University Park, PA, USA) (*DIS '06*). Association for Computing Machinery, New York, NY, USA, 140–149. <https://doi.org/10.1145/1142405.1142429>
- [25] P.T. Krein and R.D. Meadows. 1990. The Electroquasistatics of the Capacitive Touch Panel. *IEEE Transactions on Industry Applications* 26, 3 (1990), 529–534. <https://doi.org/10.1109/28.55954>
- [26] Gieran Laput, Eric Brockmeyer, Scott E. Hudson, and Chris Harrison. 2015. Acoustumtives: Passive, Acoustically-Driven, Interactive Controls for Handheld Devices. In *Proceedings of the 33rd Annual ACM Conference on Human Factors in Computing Systems* (Seoul, Republic of Korea) (*CHI '15*). Association for Computing Machinery, New York, NY, USA, 2161–2170. <https://doi.org/10.1145/2702123.2702414>
- [27] Chi-Jung Lee, Rong-Hao Liang, Ling-Chien Yang, Chi-Huan Chiang, Te-Yen Wu, and Bing-Yu Chen. 2022. NFCStack: Identifiable Physical Building Blocks That Support Concurrent Construction and Frictionless Interaction. In *Proceedings of the 35th Annual ACM Symposium on User Interface Software and Technology* (Bend, OR, USA) (*UIST '22*). Association for Computing Machinery, New York, NY, USA, Article 26, 12 pages. <https://doi.org/10.1145/3526113.3545658>
- [28] Darren Leigh, Clifton Forlines, Ricardo Jota, Steven Sanders, and Daniel Wigdor. 2014. High Rate, Low-Latency Multi-Touch Sensing with Simultaneous Orthogonal Multiplexing. In *Proceedings of the 27th Annual ACM Symposium on User Interface Software and Technology* (Honolulu, Hawaii, USA) (*UIST '14*). Association for Computing Machinery, New York, NY, USA, 355–364. <https://doi.org/10.1145/2642918.2647353>
- [29] Huaishu Peng, François Guimbretière, James McCann, and Scott Hudson. 2016. A 3D Printer for Interactive Electromagnetic Devices. In *Proceedings of the 29th Annual Symposium on User Interface Software and Technology* (Tokyo, Japan) (*UIST '16*). Association for Computing Machinery, New York, NY, USA, 553–562. <https://doi.org/10.1145/2984511.2984523>
- [30] Huaishu Peng, François Guimbretière, James McCann, and Scott Hudson. 2016. A 3D Printer for Interactive Electromagnetic Devices. In *Proceedings of the 29th Annual Symposium on User Interface Software and Technology* (Tokyo, Japan) (*UIST '16*). Association for Computing Machinery, New York, NY, USA, 553–562. <https://doi.org/10.1145/2984511.2984523>
- [31] Ivan Poupyrev, Chris Harrison, and Munehiko Sato. 2012. Touché: Touch and Gesture Sensing for the Real World. In *Proceedings of the 2012 ACM Conference on Ubiquitous Computing* (Pittsburgh, Pennsylvania) (*UbiComp '12*). Association for Computing Machinery, New York, NY, USA, 536. <https://doi.org/10.1145/2370216.2370296>
- [32] Raf Ramakers, Fraser Anderson, Tovi Grossman, and George Fitzmaurice. 2016. RetroFab: A Design Tool for Retrofitting Physical Interfaces using Actuators, Sensors and 3D Printing. In *Proceedings of the 2016 CHI Conference on Human Factors in Computing Systems* (San Jose, California, USA) (*CHI '16*). Association for Computing Machinery, New York, NY, USA, 409–419. <https://doi.org/10.1145/2858036.2858485>
- [33] Tiago Rodrigues, Prateek Dewan, Ponnurangam Kumaraguru, Raquel Melo Minardi, and Virgilio Almeida. 2013. UTrack: Track Yourself! Monitoring Information on Online Social Media. In *Proceedings of the 22nd International Conference on World Wide Web* (Rio de Janeiro, Brazil) (*WWW '13 Companion*). Association for Computing Machinery, New York, NY, USA, 273–276. <https://doi.org/10.1145/2487788.2487921>
- [34] Valkyrie Savage, Colin Chang, and Björn Hartmann. 2013. Sauron: Embedded Single-Camera Sensing of Printed Physical User Interfaces. In *Proceedings of the 26th Annual ACM Symposium on User Interface Software and Technology* (St. Andrews, Scotland, United Kingdom) (*UIST '13*). Association for Computing Machinery, New York, NY, USA, 447–456. <https://doi.org/10.1145/2501988.2501992>
- [35] Valkyrie Savage, Ryan Schmidt, Tovi Grossman, George Fitzmaurice, and Björn Hartmann. 2014. A series of tubes: adding interactivity to 3D prints using internal pipes. In *Proceedings of the 27th annual ACM symposium on User interface software and technology* (*UIST '14*). Association for Computing Machinery, New York, NY, USA, 3–12. <https://doi.org/10.1145/2642918.2647374>
- [36] Valkyrie Savage, Xiaohan Zhang, and Björn Hartmann. 2012. Midas: Fabricating Custom Capacitive Touch Sensors to Prototype Interactive Objects. In *Proceedings of the 25th Annual ACM Symposium on User Interface Software and Technology* (Cambridge, Massachusetts, USA) (*UIST '12*). Association for Computing Machinery, New York, NY, USA, 579–588. <https://doi.org/10.1145/2380116.2380189>
- [37] Valkyrie Arline Savage. 2016. *Fabbed to Sense: Integrated Design of Geometry and Sensing Algorithms for Interactive Objects*. University of California, Berkeley.
- [38] Martin Schmitz, Mohammadreza Khalilbeigi, Matthias Balwierz, Roman Lissermann, Max Mühlhäuser, and Jürgen Steimle. 2015. Capricate: A Fabrication Pipeline to Design and 3D Print Capacitive Touch Sensors for Interactive Objects. In *Proceedings of the 28th Annual ACM Symposium on User Interface Software & Technology* (Charlotte, NC, USA) (*UIST '15*). Association for Computing Machinery, New York, NY, USA, 253–258. <https://doi.org/10.1145/2807442.2807503>
- [39] Martin Schmitz, Florian Müller, Max Mühlhäuser, Jan Riemann, and Huy Viet Le. 2021. Itsy-Bits: Fabrication and Recognition of 3D-Printed Tangibles with Small Footprints on Capacitive Touchscreens. In *Proceedings of the 2021 CHI Conference on Human Factors in Computing Systems* (Yokohama, Japan) (*CHI '21*). Association for Computing Machinery, New York, NY, USA, Article 419, 12 pages. <https://doi.org/10.1145/3411764.3445502>
- [40] Martin Schmitz, Jürgen Steimle, Jochen Huber, Niloofar Dezfuli, and Max Mühlhäuser. 2017. Flexibles: Deformation-Aware 3D-Printed Tangibles for Capacitive Touchscreens. In *Proceedings of the 2017 CHI Conference on Human Factors in Computing Systems* (*CHI '17*). Association for Computing Machinery, New York, NY, USA, 1001–1014. <https://doi.org/10.1145/3025453.3025663>
- [41] Martin Schmitz, Martin Stitz, Florian Müller, Markus Funk, and Max Mühlhäuser. 2019. ...Trilaterate: A Fabrication Pipeline to Design and 3D Print Hover-, Touch-, and Force-Sensitive Objects. In *Proceedings of the 2019 CHI Conference on Human Factors in Computing Systems* (Glasgow, Scotland UK) (*CHI '19*). Association for Computing Machinery, New York, NY, USA, 1–13. <https://doi.org/10.1145/3290605.3300684>
- [42] Tatyana Vasilevitsky and Amit Zoran. 2016. Steel-Sense: Integrating Machine Elements with Sensors by Additive Manufacturing. In *Proceedings of the 2016 CHI Conference on Human Factors in Computing Systems* (San Jose, California, USA) (*CHI '16*). Association for Computing Machinery, New York, NY, USA, 5731–5742. <https://doi.org/10.1145/2858036.2858309>
- [43] Anandghan Waghamare, Youssef Ben Taleb, Ishan Chatterjee, Arjun Narendra, and Shwetak Patel. 2023. Z-Ring: Single-Point Bio-Impedance Sensing for Gesture, Touch, Object and User Recognition. In *Proceedings of the 2023 CHI Conference on*

- Human Factors in Computing Systems* (Hamburg, Germany) (*CHI '23*). Association for Computing Machinery, New York, NY, USA, Article 150, 18 pages. <https://doi.org/10.1145/3544548.3581422>
- [44] Karl Willis, Eric Brockmeyer, Scott Hudson, and Ivan Poupyrev. 2012. Printed Optics: 3D Printing of Embedded Optical Elements for Interactive Devices. In *Proceedings of the 25th Annual ACM Symposium on User Interface Software and Technology* (Cambridge, Massachusetts, USA) (*UIST '12*). Association for Computing Machinery, New York, NY, USA, 589–598. <https://doi.org/10.1145/2380116.2380190>
- [45] Sung-Yueh Wu, Chen Yang, Wensyang Hsu, and Liwei Lin. 2015. 3D-printed microelectronics for integrated circuitry and passive wireless sensors. *Microsyst Nanoeng* 1, 1 (July 2015), 1–9. <https://doi.org/10.1038/micronano.2015.13> Number: 1 Publisher: Nature Publishing Group.
- [46] Zhaobo Zhang and Xibo Yuan. 2021. Applications of Additive Manufacturing for Power Electronics Components and Converters. *IEEE Journal of Emerging and Selected Topics in Power Electronics* PP (12 2021), 1–1. <https://doi.org/10.1109/JESTPE.2021.3135285>